

## 1

## Introduction

Bin Zhu<sup>1,\*</sup> and Peter D. Lund<sup>2,\*</sup>

<sup>1</sup>Southeast University, School of Energy and Environment, No.2 Si Pai Lou, Nanjing 210096, China

<sup>2</sup>Aalto University, School of Science, P.O. Box 15100, Puumiehenkuja 2, Espoo FI-00076, Finland

### 1.1 An Introduction to the Principles of Fuel Cells

Fuel cells have been under development for more than 180 years since its discovery in the early nineteenth century. Several types of fuel cells have resulted from extensive research and development work, but only two types have reached a stage of commercialization. One is the polymer electrolyte membrane fuel cell (PEMFC) and the other is the solid oxide fuel cell (SOFC). It is a generally accepted opinion that the former is better applicable for transportation and the latter for stationary power applications. This book focuses on SOFCs ranging from traditional electrolyte-based to electrolyte-free or non-electrolyte-based devices. The focus of contents will be on materials and technologies.

Going back to the history of fuel cells, the first major step in development was the discovery of the water electrolysis to split water into hydrogen and oxygen using electricity at the beginning of the nineteenth century. Electrolysis is actually a reverse process to the fuel cell. The fuel cell principle was discovered by Humphry Davy in the early nineteenth century, which was followed by the pioneering work by Christian Friedrich Schönbein and Sir William Grove in 1838, who realized the fuel cell concept by inventing the “gas voltaic battery.” In Grove’s series of experiments on a gas battery in 1838/1839, an electric current could be produced from an electrochemical reaction between hydrogen and oxygen over a catalyst electrode couple [1]. Figure 1.1 shows the first laboratory prototype device using iron and copper sheets as hydrogen and oxygen redox electrodes (anode and cathode), and a solution of sulfate of copper and dilute acid as the electrolyte. This is very similar to a phosphoric acid fuel cell.

The term fuel cell appeared in literature first in 1889, when researchers developed coal gas, also referred to fuel gas, and coal directly as a fuel to generate electricity. Thus Grove’s gas battery was naturally named as “fuel battery” and then “fuel cell.” The fuel cell (FC) is more suitable to present Grove’s invention,

\*Corresponding authors: Dr. Bin Zhu, binzhu@kth.se; Dr. Peter D. Lund, peter.lund@aalto.fi

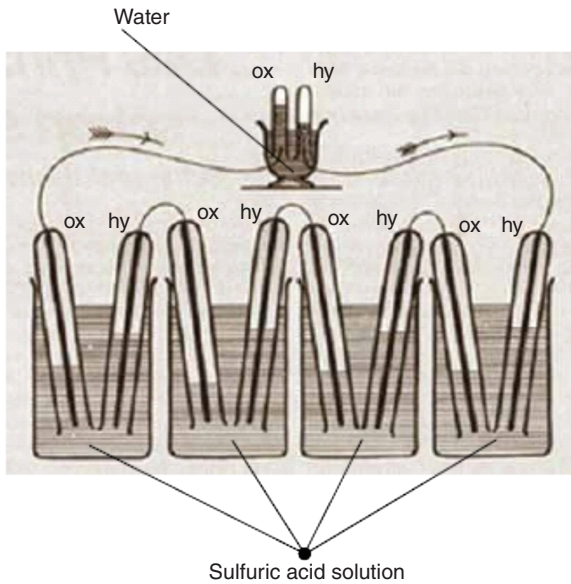


**Figure 1.1** Sketch of William Grove's 1839 fuel cell, Grove's 1839 gas voltaic battery diagram. Source: Grove 1839 [1]. Reproduced with permission of Taylor & Francis.

which also indicates its clear difference from battery energy storage due to the nature of conversion. Shortly since demonstrated in 1839 by Sir Grove, all FCs have been constructed with three functional components: anode, electrolyte, and cathode, together called the membrane electrode assembly (MEA). In all current FC technologies, the electrolyte has to be dense to prevent gas permeability [2]. The anode and cathode need hydrogen and oxygen catalysts and sufficient ionic and electronic conductivity to create fuel (e.g.  $H_2$ ) oxidation and oxidant (e.g.  $O_2$ ) reduction processes.  $H^+$  or  $O^{2-}$  ions are subsequently transported through the electrolyte to convert the fuel's chemical energy into electricity, as shown in Figure 1.2.

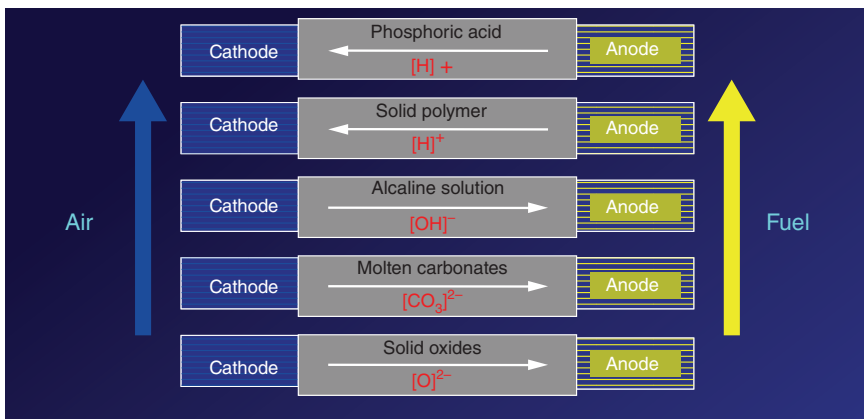


**Figure 1.2** Classical five types of electrolyte-based devices in fuel cell family.

The three-component MEA technology requires a complex FC structure and technology as all components have to be stable and compatible. The interfaces between electrolyte and anode and cathode, respectively, contribute to major polarization losses [3], while the FC delivers power, and a complex technology leads to high costs as well, delaying FC commercialization. Among the three components, the electrolyte is the key [4]. It is often called as a membrane because a fuel cell device is an assembly based on the electrolyte membrane, which acts as the separator between the anode and cathode to block electronic conduction to avoid electron short-circuiting problem. Therefore, the electrolyte is the pure ionic conductor, and any electronic conduction can make electrochemical leakage leading to losses in the device voltage and power output. On the other hand, the electrolyte must transport to support the fuel cell redox reactions, i.e. hydrogen oxidation reaction (HOR) and oxygen reduction reaction (ORR).

Several types of FCs have been developed based on the type of electrolytes, such as PEMFC based on  $H^+$  transport in a polymer electrolyte, AFC (alkaline fuel cell),  $OH^-$  ions in a solution, PAFC (phosphoric acid fuel cell) with  $H^+$  in phosphoric acid, MCFC (molten carbonate fuel cell) with  $CO_3^{2-}$  in molten carbonates, and SOFC with  $O^{2-}$  in ceramic oxides [4, 5]. The electrolyte type and its electrical properties determine which type of FC technologies and final system can be used and which energy conversion efficiency can be realized at a certain temperature. Figure 1.2 shows these five types of classical fuel cells classified by the electrolyte used.

PAFC, MCFC, and AFC have been used in different special applications: e.g. kW-sized AFC was used in Apollo's moon landing program in the 1960s and 1970s with success to produce both power and water. PAFC and MCFC were pre-commercialized in the late 1980s, and there are still ongoing MCFC commercial demonstration plants, but these technologies never reached the scale of commercialization. Only PEMFC and SOFC are left pushing toward commercialization.

## 1.2 Materials and Technologies

SOFC research and development are dominated by the yttria-stabilized zirconia (YSZ) electrolyte. In 1899 Nernst first discovered that YSZ could reach oxide ion conduction at around  $1000^\circ C$  ( $0.1 S cm^{-1}$ ). Today, the YSZ is still the choice of the electrolyte material for high-temperature SOFC. A temperature of  $800\text{--}1000^\circ C$  is typically needed for the YSZ electrolyte in order to obtain a sufficiently high ionic conductivity [6, 7], which puts major constraints to the choice of construction materials and has resulted in high costs, thus slowing the commercialization for the last decades. There has been much effort to develop alternative electrolyte materials for SOFCs to lower the operating temperature [4, 8, 9]. Examples are fluorite-structured ion-doped ceria [10], perovskite-type oxides [11],  $O^{2-}$  conducting oxides [12], and proton conducting ceramics [13] as well as other complex materials such as  $La_2Mo_2O_9$  [14], BaIn-based oxides [15], and apatite-type oxides [16]. Goodenough proposed that SOFC should be developed toward lower enough temperatures to make it technically useful [17]. His approach was to develop oxide ion conductors by design from structures based on discovered

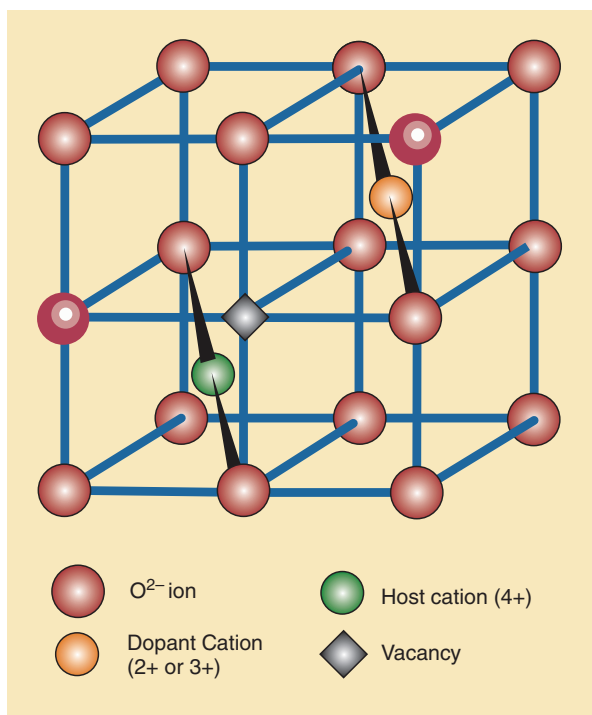


**Figure 1.3** Goodenough proposed oxide ion conductor by design: a structural method by cation doping to create oxygen vacancy. Source: Reproduced with permission from Goodenough [17]. Copyright 2000, Springer Nature.

materials. For example, the YSZ fluorite structure is presented in Figure 1.3. By using a lower valency cation, e.g.  $2+$  or  $3+$ , to replace higher valent  $Zr^{4+}$ , some oxygen vacancy must be produced in order to maintain the electrical neutrality in the crystal. In most cases, trivalent  $Y^{3+}$  is chosen to replace tetravalent ions,  $Zr^{4+}$ , to create the oxygen vacancy so that  $O^{2-}$  can move through vacancies in the Y-doped zirconia structure.

However, this approach is constrained by the structure and the objective has not yet been realized (to be discussed later). Using modern thin film technologies to reduce the thickness of the YSZ electrolyte from millimeter to meter, to even nanometer level, the electrolyte resistance and the operational temperature could be reduced. Following this, strong development efforts have been made on employing various advanced thin film technologies such as sputtering, atomic layer deposition (ALD), molecular extension growth, laser deposition, spark plasma sintering, and in situ surface nanoparticle exsolution methods, to fabricate thin film YSZ-based electrolyte. For example, Kosacki prepared a thin (down to 15 nm) film with highly textured YSZ membrane through PLD (plasma layer deposition) [18]. Surprisingly, the conductivities could be significantly enhanced to  $0.6 \text{ S cm}^{-1}$  at  $800^\circ\text{C}$  with significant low activation energy ( $E_a$ ) of 0.45 eV. This conductivity is about one order of magnitude higher than that of a conventional YSZ at this temperature. The bulk YSZ reaches  $0.1 \text{ S cm}^{-1}$  at around  $1000^\circ\text{C}$

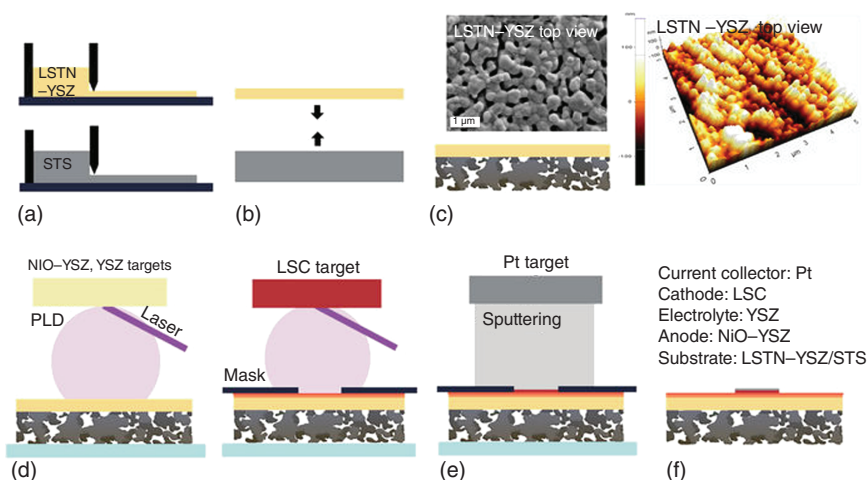


**Figure 1.4** Schematics of the fabrication process of micro-SOFC supported on LSTN-YSZ/STS substrate. (a) Tape casting. (b) Lamination. (c) Fired substrate in  $H_2$ . (d) MEA deposition. (e) Current collector deposition. (f) Micro-SOFC. Source: Kim et al. 2016 [21]. Reproduced with permission of Springer Nature.

and activation energy is around 1.0 eV. The first development of micro-SOFCs ( $\mu$ SOFCs) using the thin film YSZ membranes of 50–150 nm thicknesses was successfully fabricated using sputtering technology with the Pt electrode. The device delivered 60 and 130  $mW\ cm^{-2}$  at 350 and 400  $^{\circ}C$ , respectively [19]. The pinhole-free, composition-controllable, and conformable electrolyte membranes were fabricated by ALD technology [20]; the device operational temperature was further reduced to 265  $^{\circ}C$  while maintaining sufficient performance. These pioneering studies have in turn stimulated extensive research on nanofilms for  $\mu$ SOFCs, both from fundamental and applied perspectives. Kim et al. [21] reported some details on  $\mu$ SOFC fabrication by PLD (see Figure 1.4); achieving decent performance, the peak power density was 235, 370, and 560  $mW\ cm^{-2}$  at 450, 500, and 550  $^{\circ}C$ . Figure 1.5 displays its microstructure with a cross-sectional view of the dense YSZ around 1.5 nm in thickness.

With low temperature (LT)  $<600\ ^{\circ}C$  SOFC developments in addition to reducing electrolyte resistance by thin film technologies, another critical issue arises involving insufficient kinetic process and catalyst function leading to especially slower ORR for the cathode reaction and power output. This is actually a limiting factor to determine the device performance and efficiency for low temperature operations. To overcome the sluggish kinetics from the electrodes, especially to minimize the cathodic polarization loss and enhance the ORR, to enable the device sufficient efficiency and power output, most research and development have been focused on new functional cathode materials together with microstructure controlling in the device fabrications. Various effects on the microstructure include the composition, particle and pore sizes and their distributions, particle connections, porosity, tortuosity, specific surface area, ionic and electronic conductivities, electrode thickness, and interfacial bonding, which are noted for research and development of a new cathode material,

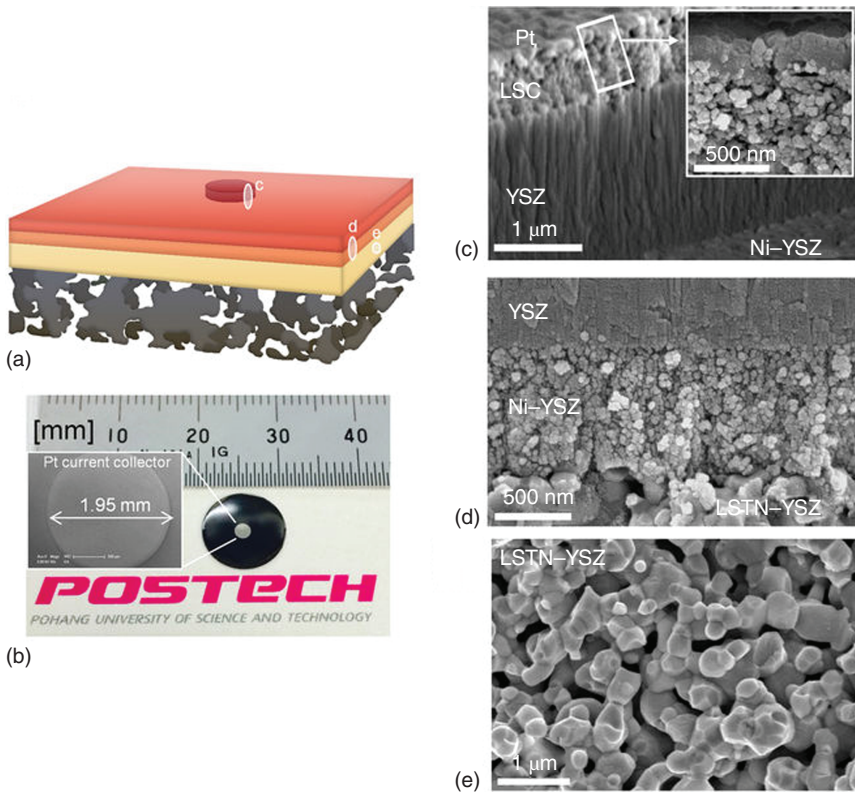


**Figure 1.5** Image of micro-SOFC. (a) Schematic of a thin film MEA supported on porous STS substrate. (b) Photograph of a cell. A logo is a trademark of Pohang University of Science and Technology (POSTECH) and is protected by copyright; it is used in this figure with permission. Cross-sectional SEM image of (c) Pt/LSC/YSZ (Inset: magnified view of Pt/LSC), (d) YSZ/Ni-YSZ/LSTN-YSZ, and (e) LSTN-YSZ contact layer. Source: Kim et al. 2016 [21]. Reproduced with permission of Springer Nature.

especially below 600 °C [22, 23]. Perovskite-structured oxides,  $ABO_3$ , as shown in Figure 1.6, have been used successfully [24].  $La(Mn/Co)O_3$  based on A-site and B-site doping by rare earth, alkaline earth, and transition elements are successful examples of high performance, more durable and comparable with other SOFC device components.

A-cations are located in every hole, which is created by eight  $BO_6$  octahedra, as shown in Figure 1.6, thus having a 12-fold coordinate site, and the B-cations in 6-fold oxygen coordination. There are many  $ABO_3$  compounds for which the ideal cubic structure is distorted to a lower symmetry (e.g. tetragonal, orthorhombic, etc.). Oxygen vacancies can be created by ionic doping within the perovskite structure, similar with fluorite structure. Ion doping effect can create an impact on both electron and ion transport. One of the best perovskite cathodes for low-temperature solid oxide fuel cells (LTSOFCs) is  $Ba_{0.2}Sr_{0.8}Co_{0.6}Fe_{0.4}O_3$  [25]; its electronic and oxygen ionic conductivities at 600 °C are 200 and  $0.1 \text{ S cm}^{-1}$ , respectively.

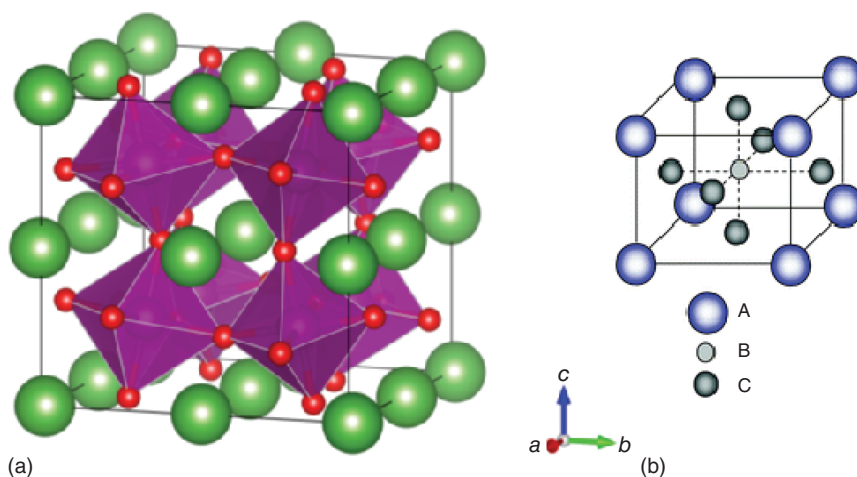


**Figure 1.6** Perovskite structure oxides for functional LSOFC cathode catalyst material. In  $ABO_3$ , there are (a) corner-sharing ( $BO_6$ ) octahedra with A ions located in 12-coordinated interstices and (b) B-site cation at the center of the cell. Source: Kan et al. 2016 [24]. Reproduced with permission of Royal Society of Chemistry.

Other types of perovskite structure oxides have been also developed for LSOFCs. A typical example is double perovskites,  $Sr_2FeMoO_6$  (SFM) [26], because the unit cell is twice that of perovskite. It has the same architecture of 12-coordinate A sites and 6-coordinate B sites, but two cations are ordered on the B site. In the case of  $Sr_2FeMoO_6$ , the Fe and Mo atoms are ordered in a 3D chessboard-type fashion. Also, the ratio between Fe and Mo can make a significant effect on electrical and catalyst functions. Typically,  $Sr_2Fe_{1.5}Mo_{0.5}O_{6-\delta}$  ( $SF_{1.5}M_{0.5}$ ) has been reported for remarkable electrical conductivity of  $550 \text{ S cm}^{-1}$  in air and  $310 \text{ S cm}^{-1}$  in hydrogen at  $780^\circ\text{C}$ , as one of the best redox stable electrodes for LSOFCs; this makes it available for both anode and cathode materials in SOFCs. In the case of SFM0.5 as the anode and cathode to construct a symmetrical SOFC, the device has achieved a peak power density of over  $835 \text{ mW cm}^{-2}$  at  $900^\circ\text{C}$  using  $H_2$  as fuel and ambient air as the oxidant [26].

The SFM shows also a good catalyst for oxidation of hydrocarbon fuel operation, e.g. direct oxidation methanol using the SFM0.5 as the anode and perovskite and  $Ba_{0.5}Sr_{0.5}Co_{0.8}Fe_{0.2}O_3$  (BSCF) as the cathode based on perovskite ionic electrolyte,  $La_{0.8}Sr_{0.2}Ga_{0.83}Mg_{0.17}O_3$  to construct the all perovskite SOFC device, in a configuration of  $SF_{1.5}M_{0.5}/La_{0.8}Sr_{0.2}Ga_{0.83}Mg_{0.17}O_3$ (electrolyte)/BSCF. This device obtained a maximum power density of  $391 \text{ mW cm}^{-2}$  at  $800^\circ\text{C}$  [27].

In addition to perovskite cathodes, other transition metal oxides are also efficient for low temperature operations, typically nickel oxide, iron oxide, cobalt oxide and their composites, or lithiated oxides, such as lithiated or Li compound layer structure oxides, such as  $Li_xM$  ( $M = Ni, Fe, Co$ ) $O_2$ . These oxides have shown much effective catalyst functions due to its great proton conductivity, so far the best of proton ceramic materials,  $0.1 \text{ S cm}^{-1}$  at  $500^\circ\text{C}$  [28], and other unique advantages, e.g. triple charge carriers of  $H^+$ ,  $O^{2-}$  and  $e^-$  as shown in Figures 1.7 and 1.8 [29, 30].

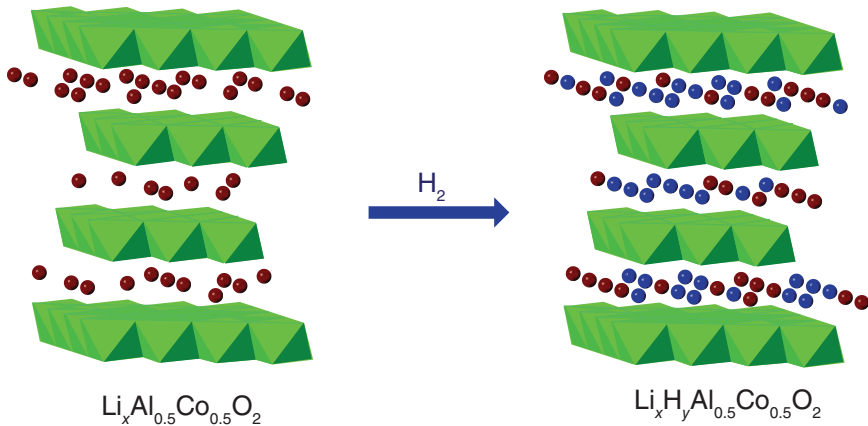


**Figure 1.7** Layer structure reported having the highest proton conductivity  $0.1 \text{ S cm}^{-1}$  at  $500^\circ\text{C}$ . Source: Reproduced with permission from Lan and Tao [28]. Copyright 2014, John Wiley & Sons.

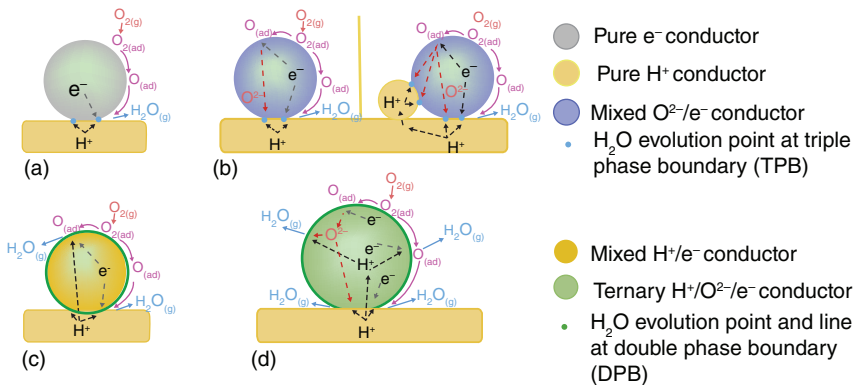


**Figure 1.8** Triple charge transfer in LTSOFC cathode and schematic illustrations of the oxygen reduction and water generation pathways in various cathodes: (a) pure electronic conductor; (b) mixed  $\text{O}^{2-}/e^-$  conductor (mixed electronic and ionic conductor [MIEC], left) and MIEC composited with  $\text{H}^+$  conducting oxide (right); (c) mixed  $\text{H}^+$  and  $e^-$  conductor (mixed proton and electron conductor [MPEC]) and (d) triple-conducting ( $\text{H}^+/\text{O}^{2-}/e^-$ ) oxides. Source: Reproduced with permission from Fan and Su [29]. Copyright 2016, Elsevier.

Figure 1.8 displays the layer structure of  $\text{LiNi}_{0.8}\text{Co}_{0.2}\text{O}_2$  with a triple ( $\text{H}^+/\text{O}^{2-}/e^-$ ) conducting catalyst material. The triple charge conducting material can speed up the cathodic ORR process, to reduce significantly the cathodic polarization, thus enhancing the device performance.

### 1.3 New Electrolyte Developments on LTSOFC

As proposed by Goodenough, new materials need to be developed to replace YSZ [19] to make SOFC operational at low enough temperatures. This means

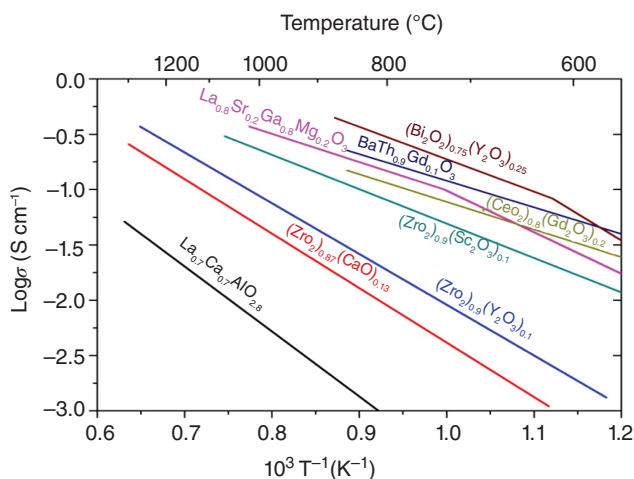
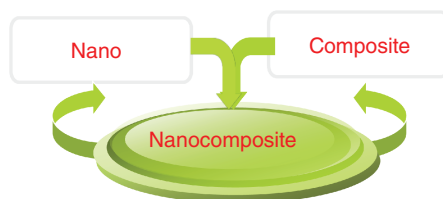


**Figure 1.9** Temperature dependence of conductivities for various oxide electrolytes from *High-Temperature Solid Oxide Fuel Cells: Fundamentals, Design, and Applications* by S.C. Singhal and K. Kendall (Eds.). Publisher: Elsevier Science (2004). Source: Reproduced with permission from Singhal and Kendall [31]. Copyright 2003, Elsevier.

that alternative electrolytes should be designed for low temperatures; commonly accepted temperature is below 600 °C for LTSOFC. Therefore, new electrolyte materials should reach an ionic conductivity of  $0.1 \text{ S cm}^{-1}$  < 600 °C. Following this direction, worldwide LTSOFC movement has been conducted to look for new electrolyte materials. However, no alternative to be good enough to compete with YSZ on overall requests has not yet been found. Figure 1.9 displays some of the new electrolyte materials developed in this line.

It can be seen from Figure 1.9 that almost no alternative oxide electrolyte materials can reach  $0.1 \text{ S cm}^{-1}$  below 600 °C. Though  $\text{Bi}_2\text{O}_2\text{-Y}_2\text{O}_3$  is used at this level, it could not be used for SOFCs due to its direct reduction to Bi metal in fuel cell operation, thus the loss of the ionic conduction. Another approach to develop new electrolyte materials based on surface and interfacial ionic conduction is also published in Nature in the same year of Goodenough' structural doping [32]. To obtain the interfacial high ionic conductivity, nano and composite, so-called nanocomposite, approach has been demonstrated to be more effective. A very successful case may be exemplified by ceria-based two-phase composite materials [33–36]. Such materials have been found very functional for LTSOFCs between 300 and 600 °C. Figure 1.10 presents a schematic drawing for such a methodology.

**Figure 1.10** Combining nano and composite approach to develop effective new functional electrolyte materials for LTSOFC.



On one hand, nanotechnology can create high surface area and active sites with defects for high ionic transportation thus to enhance the ionic conductivity; on the other hand, the composite approach can enhance the nanomaterial stability and further enhance the ionic conduction by the interfacial mechanism. Therefore, the nanocomposite approach can be very effective to develop high ionic conductors for LT-SOFC electrolyte demands. Ceria has a stable fluorite structure as YSZ by Ce to replace Zr with a wider range of dopants than that in zirconia. Using rare earth element doping, e.g. samarium, gadolinium, and yttrium, doped  $\text{CeO}_2$  have high expectation to replace YSZ because its  $\text{O}^{2-}$  conductivity can reach the same level,  $0.1 \text{ S cm}^{-1}$  at  $800^\circ\text{C}$ , i.e.  $200^\circ\text{C}$  lower than that of YSZ. However, except good ionic conductivity at a lower temperature, many other aspects are not as good as with YSZ. For example, in fuel cell-reduced atmosphere,  $\text{Ce}^{4+}$  can be reduced to  $\text{Ce}^{3+}$ , which results in direct electronic conduction and short-circuiting problem and thus in a significant loss in device voltage and power output; with  $\text{Ce}^{4+}$  to  $\text{Ce}^{3+}$  reduction, the big atom volume change causes microcracking and leads to gas leakage and finally the device invalid during the fuel cell operation. Even more,  $0.1 \text{ S cm}^{-1}$  can occur only at  $800^\circ\text{C}$ , still not sufficient for LT ( $<600^\circ\text{C}$ ). These challenges have made ceria itself not yet successful for the alternative electrolyte and SOFC technologies. To realize ceria-based electrolytes, a more effective way is to develop ceria-based composite electrolytes [36] as illustrated in Figure 1.10, which have been extensively investigated and demonstrated by excellent performances for SOFCs at LTs. Among various ceria-based composite materials, ceria-carbonate two-phase composites have been most widely investigated as new electrolytes with successful applications in LT,  $300\text{--}600^\circ\text{C}$  SOFCs [33–37]. Hybrid proton and oxygen ionic conduction and even triple ions ( $\text{H}^+/\text{O}^{2-}/\text{CO}_3^-$ ) transport processes have been studied and reported with excellent fuel cell performances [36, 38–41].

Figures 1.11 and 1.12 present hybrid and triple ion transport fuel cell devices based on ceria-carbonate composite electrolytes.

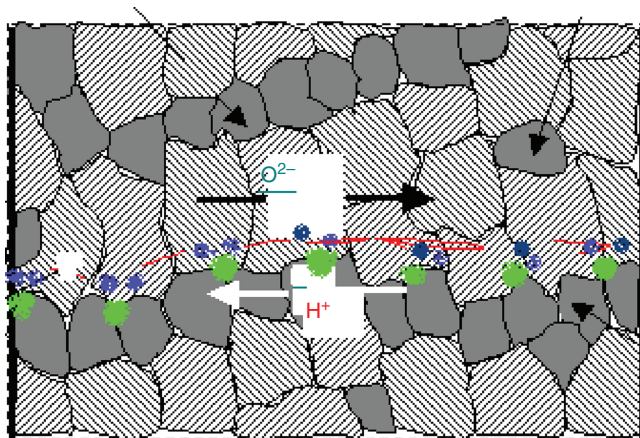


**Figure 1.11** Hybrid  $\text{H}^+/\text{O}^{2-}$  conduction in the ceria-based composite electrolyte. Source: Zhu 2006 [36]. <http://www.electrochemsci.org/ESG.htm>. Licensed Under CC BY 4.0.

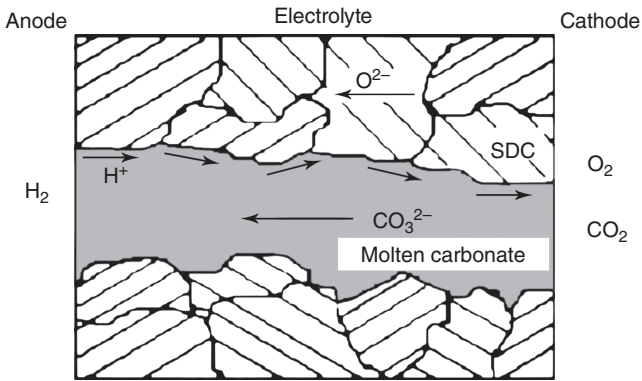


**Figure 1.12** Triple ion transport mechanism in the ceria-carbonate composite electrolyte. Source: Reproduced with permission from Xia et al. [39]. Copyright 2009, Elsevier.

The  $O^{2-}$  conduction in ceria phase is determined by the oxygen ion vacancies (a mechanism) in the ceria lattice;  $H^+$  conduction may be produced by the formation of bonding with the carbonate through temporal bonding,  $H^+ - CO_3 = (HCO_3^-)$  mechanism. Both  $H^+$  and  $O^{2-}$  conduction can be integrated into one composite to enhance the system conductivity based on the composite effect. This effect concerns the ion conduction at interfaces, or interfacial conduction, as the key. Figure 1.11 presents a schematic for such hybrid proton and oxygen ion conduction model and depicts also the hybrid/dual  $H^+/O^{2-}$  conduction routes and the conducting chain:  $H \cdots O - H$ ,  $H - O - H$  and  $O - H \cdots O$  atoms/ions. This refers to an interfacial conducting path/mechanism for the  $H^+$  (marked by two small bolls/dots in Figure 1.11) and  $O^{2-}$  (larger boll).

In Figure 1.12, a triple ion transport mechanism has been proposed by Xia et al. [39]. They introduced some  $CO_2$  in the ceria-carbonate electrolyte fuel cell and operated above the carbonate melting point, achieving  $1700 \text{ mW cm}^{-2}$  at  $650^\circ\text{C}$ , the best performance of the ceria-carbonate electrolyte fuel cells. They proposed triple-charge transport mechanism to interpret such excellent performance, presented in Figure 1.12.

Because  $H^+$  and  $O^{2-}$  ions are fuel cell source ions, hybrid  $H^+/O^{2-}$  conduction can enhance the device charge carrier concentration resulting in higher current and thus power outputs.  $1150 \text{ mW cm}^{-2}$  has been achieved at  $490^\circ\text{C}$  [42], while in triple ionic process, by adding one more source ion of  $CO_3^{2-}$ , the fuel cell device reached  $1700 \text{ mW cm}^{-2}$  at  $650^\circ\text{C}$ . More interestingly, the ceria-carbonate fuel cell can be developed in various electrochemical operation modes as SOFC, MCFC, or joint SOFC/MCFC [43].

Successful hybrid ionic conducting composite electrolyte materials for LTSOFCs may also be highlighted by heterostructure, which can be prepared by directly using proton and oxide ion-conducting oxides in the composite. Zhu and Schober first presented such a hybrid system based on BZY ( $BaZr_{0.8}Y_{0.2}O_{3-d}$ ) proton-conducting perovskite with samarium-doped ceria (SDC), a fluorite structure with oxide ion conductor composite. This novel composite system composed of the proton and oxide ion-conducting oxides successfully demonstrated

a fuel cell device reaching  $250 \text{ mW cm}^{-2}$  at  $550^\circ\text{C}$  [44]. Following this route, high sintering temperature at  $1550^\circ\text{C}$  was employed for BZY/SDC composite system, which produced a new perovskite phase of  $\text{BaCe}_{1.6}\text{Y}_{0.2}\text{Gd}_{0.2}\text{O}_{4.9}$  (BCYG) between SDC and BZY phases. As reported such a new phase, BCYG displayed ionic conductivity higher than that of constituent BZY and SDC materials. This new composite system was applied as the electrolyte for the fuel cell to achieve  $657 \text{ W cm}^{-2}$  at  $700^\circ\text{C}$  [45]. This system suggests that the BZY–SDC two-phase composite may be transferred to three-phase by high temperature heat treatment, while the intermediate phase formed between two constituent phases still dominated the ionic conductivity and transport in such composite material. But the ionic transport mechanism is not very clear to demand further investigation. For example, either  $\text{H}^+$  or  $\text{O}^{2-}$  or both may be transported in this newly formed BCYG phase. The basic phenomenon still belongs to ionic transport in the composite and heterostructure materials.

Two phases based on proton and oxide ion-conducting oxides may make several ways for ionic transportation,  $\text{H}^+$  and  $\text{O}^{2-}$  transport individually in respective proton and oxide ion phases, and more significantly, superionic conduction through interfaces between two constituent materials as ionic highways, as shown in Figure 1.13.

In order to develop alternative YSZ electrolyte materials with sufficient ionic ( $\text{H}^+$ ,  $\text{O}^{2-}$  or hybrid) conductivities, say,  $0.1 \text{ S cm}^{-1}$ , the nanocomposite presented another powerful way by designing interfaces and interfacial superionic conduction between two phases of the heterostructure composite. Such an approach called multifunctional nanocomposite for advanced fuel cells (nanocomposites for advanced fuel cells [NANOCOFC], [www.nanocofc.com](http://www.nanocofc.com)) focusing on advanced material and functionalities design on interfaces; see Figure 1.14. In such composite structure, two constituent phases may have moderate ionic conductivity, or more often with one insulating phase, e.g. an insulating oxide;

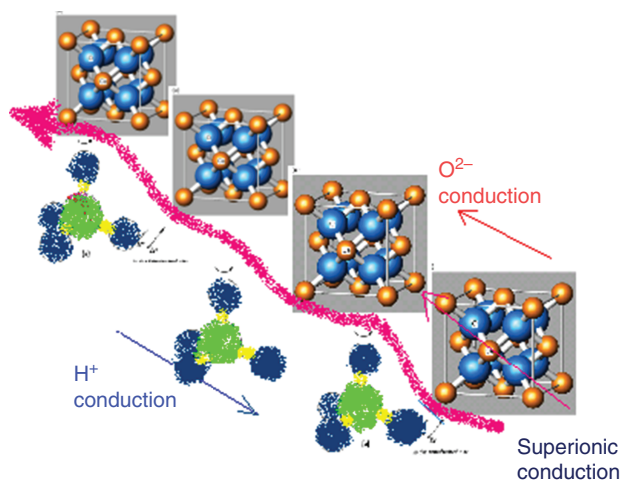


**Figure 1.13** Proton, oxide ion paths in respective proton and oxide ion conducting phase and interfacial ionic highways.

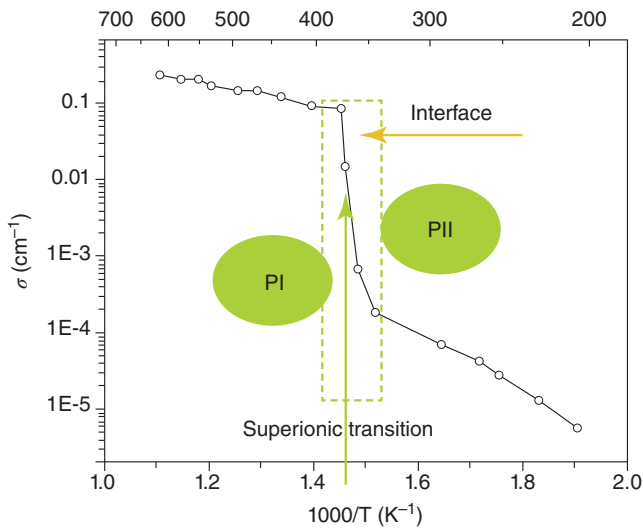


**Figure 1.14** Superionic transition at two constituent phases' interfaces in the composite materials.

a much high ionic conductivity with a great enhancement compared to the constituent phase can be produced between the two-phase contacting regions, i.e. interfaces. This is so-called interfacial superionic conductivity. It should be pointed out that such conduction mechanism does not involve any material structural changes, but only changes in the interface due to microstructures and interactions between two phases.

A theoretical calculation has been carried out between ceria and carbonate composite electrolyte indicating the existence of the interfacial ionic highways. A model presented in Figure 1.15 based on coulombic interaction points out there are very low activation energies for ionic transport, 0.2 eV for  $O^{2-}$  and 0.1 eV for  $H^+$  transport, respectively [46].

According to the Arrhenius relation,  $\sigma = \sigma_0 \exp(-\varepsilon_a/kT)$ , the interfacial ionic transport design is very favorable to develop superionic conductors because the interfacial mechanism is favorable by optimizing all parameters to promote high ionic conductivity from the following aspects:

- (i) *High mobile ion concentration,  $n$  ( $\sigma_0$ ).* It is directly proportional to the ionic conductivity value level, while at interface or particle surfaces, high defects can be created without structural factor limitations. But in structural doping approach, it is often a limiting factor, e.g. only 8% yttrium allowed to stabilize cubic fluorite structure, YSZ within zirconia.
- (ii) *Low activation energy,  $\varepsilon_a$ .* The ionic migration activation energy is more effective to determine conductivity due to ionic conductivity dependence being a reciprocally exponential function. Interfacial paths have no strong bond energy to break in order to activate ion mobile, thus requiring much lower activation energy compared that of the ion mobility in the structure.

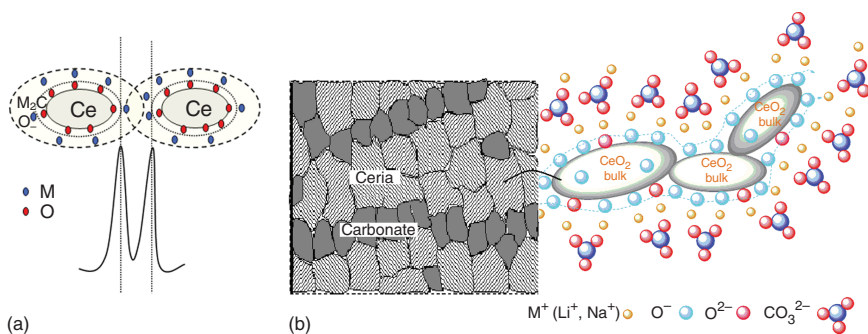


**Figure 1.15** Interfacial superionic ( $H^+$  and  $O^{2-}$ ) conducting paths in ceria–carbonate composite electrolyte. (a) Interactions and potential between the oxygen ions on the ceria particle and  $M^+$  ( $Li^+$ ,  $Na^+$ , or  $K^+$ ) cations of the carbonate, and electrical field in the interfaces between two constituent phase particles. (b) The oxygen ions on the ceria particles and interactions with cations of the carbonates may essentially consist of conducting highways/paths at interfaces of the two-phase materials, resulting in interfacial superionic conduction. Source: Reproduced with permission from Zhu et al. [46]. Copyright 2008, Elsevier.

(iii) *Long ionic transport path,  $L$  ( $\sigma_0$ )*. This effect is again proportional to conductivity. While ions transport at interfaces, one-step jump distance is from particle to particle through surface defects. Such jumping step length is in nanometer level for nanocomposites or even longer. But in structure design, defects are created within the structure unit cell, which is in angstrom level, i.e. ions jumping steps between lattice units from cell to cell in angstrom level, even less, because based on Einstein–Nernst equation, 1/6 probability is allowed for directional mobility driven by an external electrical field. In this case, interfacial conduction has no such limit because three-dimensional interfaces can be constructed on particles, which can adjust transport paths directed by the driven field.

From the above analyses, we can see the more advanced material design on interfacial superionic conductivity with all optimized parameters indicated by Arrhenius relation than that of the ion-doped structural design. Such interfacial approach has demonstrated a great ionic conductivity,  $0.1 \text{ S cm}^{-1}$  at  $300^\circ\text{C}$ , first reported by Wang et al. in a ceria–sodium carbonate core–shell structure composite; see Figure 1.16 [47].

Wang et al. proposed the “Swing” model to describe proton pathway and transport process; see Figure 1.17 for the SDC/ $Na_2CO_3$  composite system. This is essentially an interfacial conduction mechanism. Proton can transport in the carbonate–SDC contact region, i.e. interface, through  $CO_3^-$  anion bonding to form temporal  $HCO_3^-$ , which can be transferred through one carbonate anion to another.

The interfacial ionic conduction mechanisms have been further investigated by Shalima and Gulgun [48], who proposed the interfacial ion transport model shown in Figure 1.18. Core–shell structured SDC particles are connected by carbonate networks.

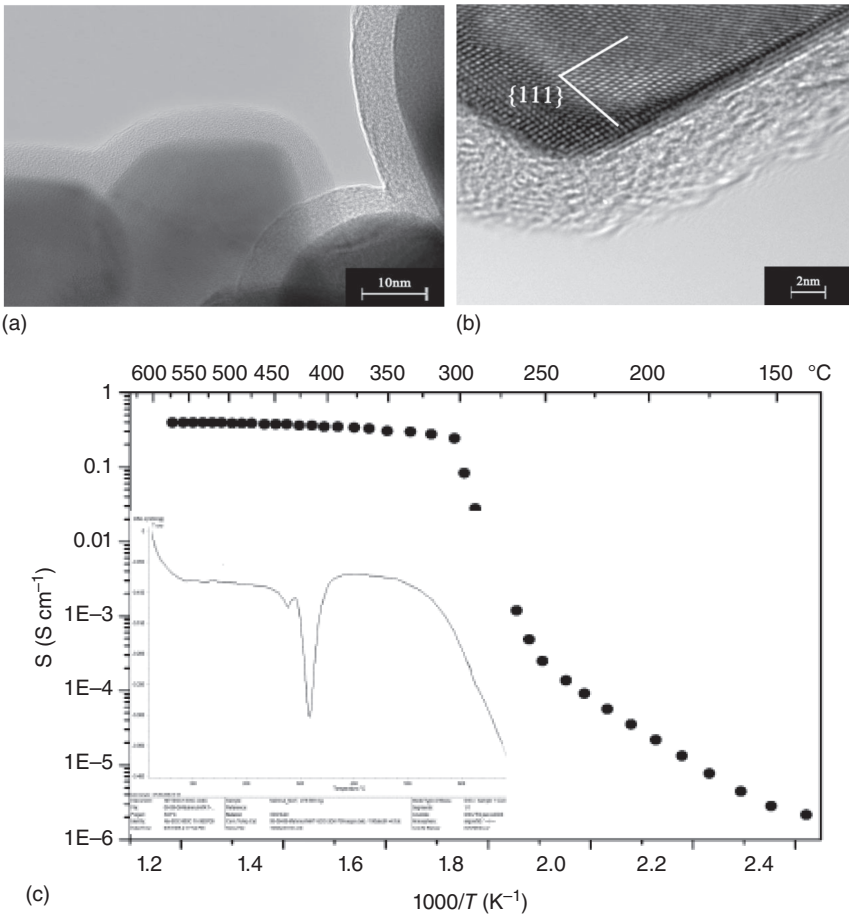


**Figure 1.16** Superionic phase transition below 300  $^{\circ}\text{C}$  in core-shell structure of  $\text{Na}_2\text{CO}_3$ -SDC composite. (a) TEM image and (b) HRTEM image of as-prepared SDC/ $\text{Na}_2\text{CO}_3$  nanocomposite; (c) temperature dependence of conductivities for as-prepared core-shell SDC/ $\text{Na}_2\text{CO}_3$  nanocomposite inserted by a DSC curve of as-prepared SDC/ $\text{Na}_2\text{CO}_3$  sample. Source: Reproduced with permission from Wang et al. [47]. Copyright 2008, Elsevier.

This composite approach was further extended to optimize hybrid ionic–electronic conductivity in two-phase ceria–zirconia composite with cobalt oxide and  $\text{Na}_2\text{CO}_3$  as suitable additives [50]. Interfacial  $\text{O}^{2-}$  conduction was proposed through carbonate intermediate layer between YSZ particles as shown in Figure 1.19.

Moreover, the heterostructure composite approach has been also applied to include semiconductor with ceria ionic conductor, e.g. a p-type  $\text{LiZnO}_2$  semiconductor, and reduced ceria as an n-type when in the fuel cell or hydrogen environment. In this case, a redox reaction can take place between p- $\text{LiZnO}_2$  and n-reduced ceria, as shown in Figure 1.20: i.e. an electron combination process may occur. The electrons can be transferred from n-ceria particle to p- $\text{LiZnO}_2$ , resulting in the absence of net electrons to cause electronic conduction within

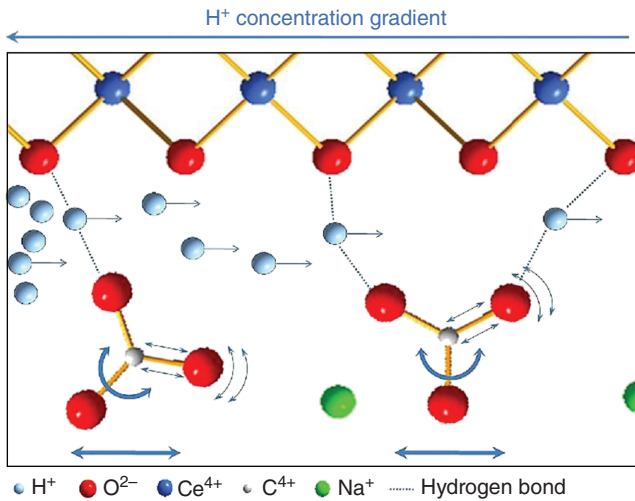


**Figure 1.17** Swing model to describe proton transport through carbonate and ceria interface from Xiaodi Wang, PhD thesis, KTH. Source: Reproduced with copyright permission.

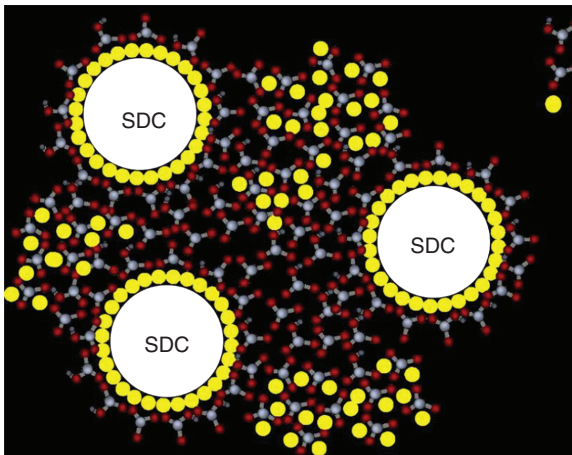


**Figure 1.18** Ceria-carbonate nanocomposite transport model. Source: Reproduced with permission from Wang et al. [49]. Copyright 2011, Elsevier.

this novel n–p semiconductor–ionic heterostructure. This provides a useful and novel methodology of electrolytes–nanocomposites for net electron free through extracting e–conduction by the n–p heterostructure to develop superionic conductors.

In parallel, there have been strong research activities on semiconductor–ionic heterostructure composites, e.g. semiconductor  $\text{SrTiO}_3$  (STO) with a fluorite structure such as in YSZ ionic electrolyte. Several orders of the magnitude for ionic conductivity enhancement were discovered for such semiconductor–ionic heterostructure nanocomposite [53]. This has been debated. For example, X. Guo in a comment on “Colossal ionic conductivity at interfaces of epitaxial  $\text{ZrO}_2\text{:Y}_2\text{O}_3/\text{SrTiO}_3$  heterostructures” [54] argued that the observed great conductivity actually came from the  $\text{SrTiO}_3$  electronic conduction.

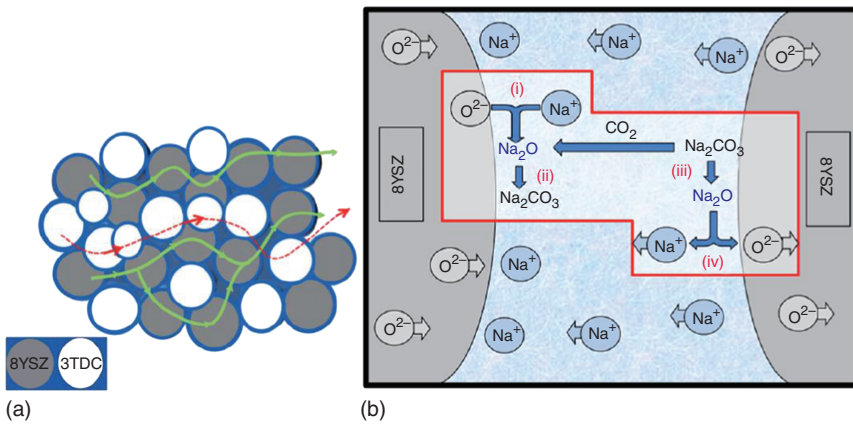
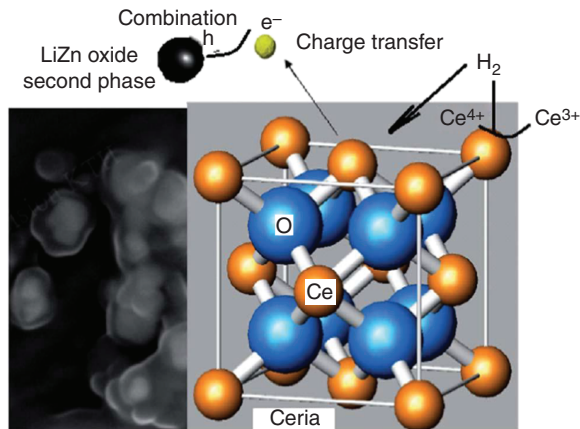


**Figure 1.19** Interfacial ionic conduction is presented in YSZ–carbonate composite system. (a) Two material particles for 3YSZ and 8YSZ in the composite. (b) Schematic representation of overall  $\text{O}_2$  conduction in composites. Solid green lines show the oxygen transporting paths and red dots represent the electron transporting path. (c) Schematic diagram representing the oxide ion conduction *via* hopping through  $\text{Na}^+$  ions in percolation layer. Source: Reproduced with permission from Maheshwari and Wiemhöfer [51]. Copyright 2016, Elsevier.

**Figure 1.20** Semiconductors n–p heterostructure extraction e-conduction. Source: Fan et al. 2014 [52]. Adapted with permission of Royal Society of Chemistry.



Though there is a big debate that it does not affect this new discovery with a great significance: i.e. interfaces play the key role in ionic conduction in such ion/semiconductor  $\text{ZrO}_2\text{:Y}_2\text{O}_3/\text{SrTiO}_3$  heterostructure composite. It has been highly expected for  $\text{YSZ}/\text{SrTiO}_3$  heterostructure composite as a breakthrough in the electrolyte research and development with “a profound effect on use in oxide ion conductors for SOFCs leading to exciting new technologies” [55]. However, the  $\text{YSZ}/\text{STO}$  has not yet been used as an alternative electrolyte to replace YSZ though a great ionic conductivity enhancement was indeed observed than that of YSZ. It may be due to the existence of electronic conduction from the semiconductor STO and electronic conduction could not be avoided as commented by Guo. According to fuel cell science, the electrolyte should have pure ionic

transport, any electronic conduction may cause significant losses in the device voltage and power.

## 1.4 Beyond the State of the Art: The Electrolyte-Free Fuel Cell (EFFC)

SOFC electrolytes have been developed for a long time, some alternatives have emerged, but still the original YSZ material dominates commercial development of SOFC. A well-justified question is if a SOFC could be realized by an alternative way. A commonly chosen approach has been to reduce the electrolyte thickness. Another intriguing approach may be to eliminate the traditional electrolyte and replace it with something more innovative. The single-component/layer fuel cells or the electrolyte-free fuel cell (EFFC) may be an example of such development demonstrated for the first time in 2011. Zhu et al. made the first single-component EFFC invention [56–59] shown in Figure 1.21.

This development is the major focus of Part II of this book. Recently, many publications have supported the single-component fuel cell devices using semiconductors of perovskite or layer-structured transition metal oxides as the functional layer in a single layer fuel cell configuration. The fuel cell functionality is realized through novel semiconductor ionic materials (SIMs).

A joint effort involving 15 organizations including industries from Europe and Asia has been initiated [60].  $\text{LiCoAlO}_2$  [28],  $\text{SmNiO}_3$  [61], and  $\text{LaSrCaTiO}_3$  [62] semiconductor materials undergo a protonic conducting phase transition under fuel cell operation and perform as good as a conventional electrolyte. Being different from the conventional electrolyte design by ion substitution to create oxygen vacancies or defects, new properties arise from strong correlations

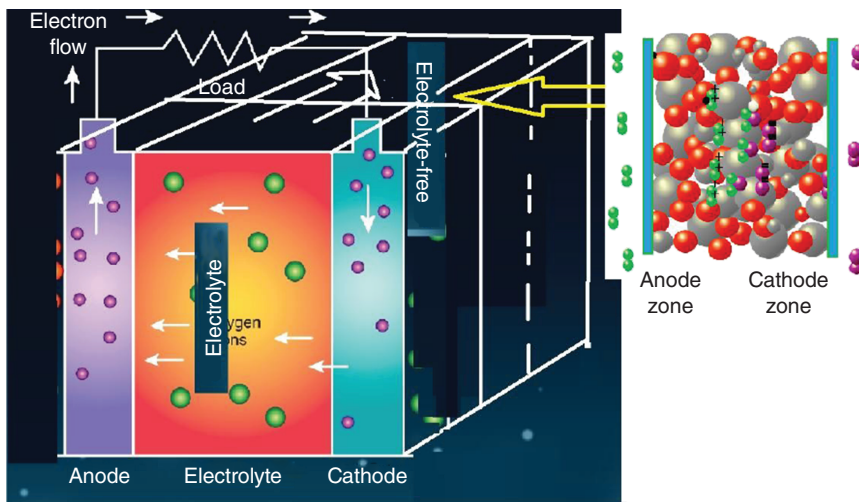
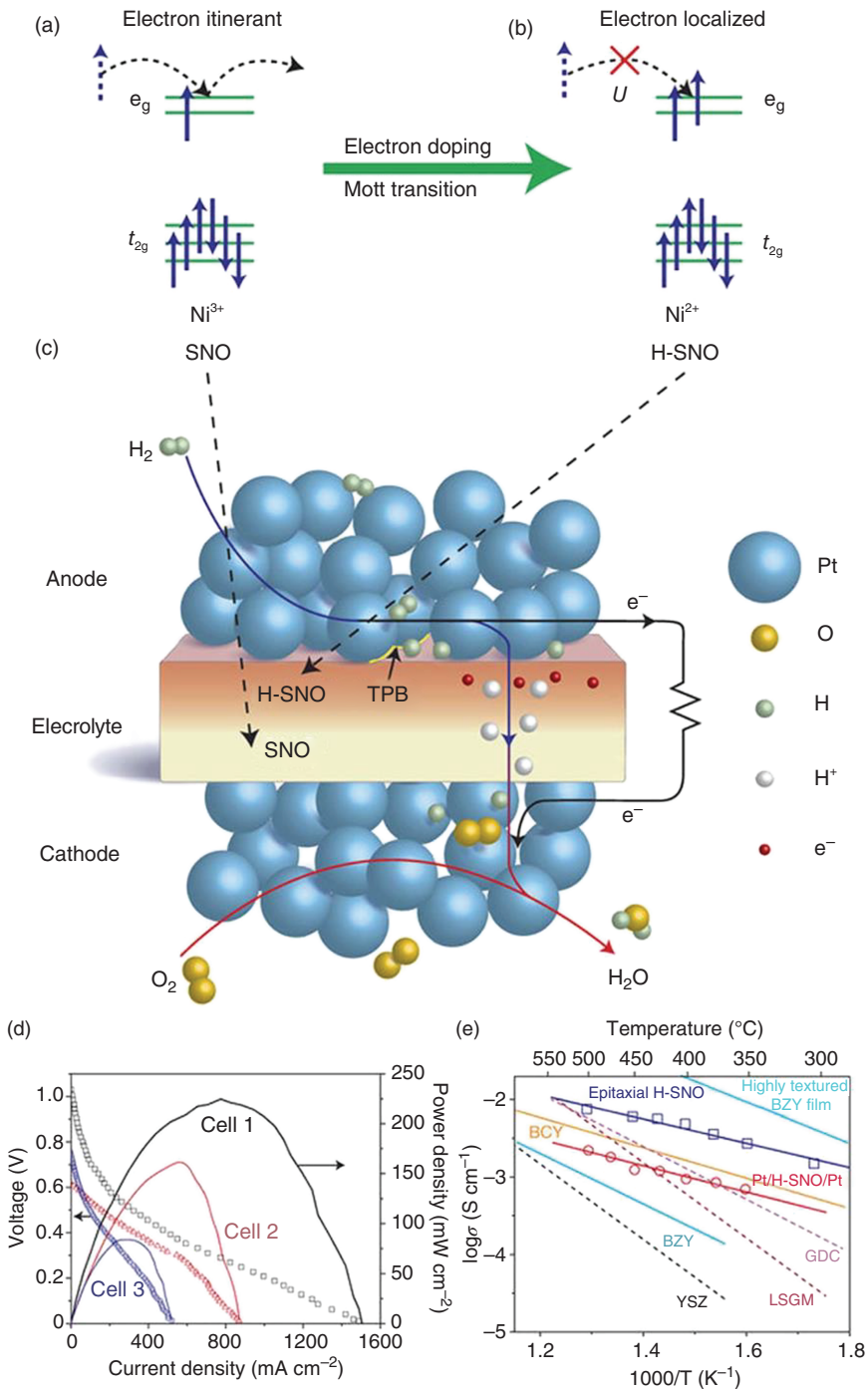


Figure 1.21 From electrolyte based on electrolyte layer-free fuel cell device.

between electron and electron or electron band and ion. To develop ionic properties through semiconductors has effectively extended the electrolyte and electrode material selections for advanced LTSOFCs and certainly explored the new fundamental understanding of research and development on fuel cell materials and technologies.

Based on extensive research and development in this single-component/layer or EFFCs, new functional materials have been discovered based on the semiconductor or semiconductor–ionic properties. Semiconductors and semiconductor–ionic heterostructure materials could play an important role in advanced LTSOFCs as well as in realizing the device functions. Three categories of the semiconductor–ionic materials may be identified: (i) single-phase semiconductors, e.g. perovskite and layered structured oxides,  $\text{SmNiO}_3$ ,  $\text{SrTiO}_3$ , and  $\text{LiCoAlO}_2$ ,  $\text{LiNiFeO}_2$ ,  $\text{LiNiCoO}_2$ , etc (ii) semiconductor–ionic two phase composite materials (iii) insulating type wide bandgap semiconductors. More semiconductor oxides, e.g.  $\text{ZnO}$ , have been also discovered very lately to be transformed to semiconductor–ionic functions. In transition metal semiconductor oxides, strong electron correlations can induce some special properties, e.g. metal–insulation transition, i.e. Mott transition materials.  $\text{SmNiO}_3$  perovskite is a typical example of such correlated transition of electrical conduction. Zhou et al. [61] prepared a thin film of metal conducting  $\text{SmNiO}_3$  (SNO) with an initial electrical conductivity of  $1000 \text{ S cm}^{-1}$ , which can be applied as an electrolyte in LTSOFCs below  $500^\circ\text{C}$  (Figure 1.22). They prepared an SOFC device based on  $1.5 \mu\text{m}$  thick SNO electrolyte. With Pt electrodes, this device delivered an open-circuit voltage (OCV) of  $1.03 \text{ V}$  and a maximum power density of  $225 \text{ mW cm}^{-2}$  at  $500^\circ\text{C}$  (Figure 1.22d). They proposed a high proton-conducting H-SNO material transformed from SNO in fuel cell operation, thus resulting in good fuel cell performance. They also found the low ionic activation energy,  $E_a$  for the H-SNO compared to the other best  $\text{O}^{2-}$  and  $\text{H}^+$  conducting electrolytes, as shown in Figure 1.22e.

The transition from the electronic conductor to extrinsic proton/ionic conductor, which is also reported in other works [28, 52, 61, 63] to be promising electrolyte materials for LT-SOFCs. These semiconductors have shown a common property: i.e. in fuel cell operations they can experience a transition from semiconductor electronics to ionic conduction. Most commonly, semiconductor–ionic materials are developed based on two-phase materials consisting of one semiconductor and one ionic material, so-called semiconductor and ionic heterostructure composites. In this case, both electron and ionic conduction may coexist in the material. Interestingly, such mixed electronic and ionic conduction materials can replace the electrolyte to build the fuel cell devices, so-called semiconductor–ionic membrane fuel cells (SIMFCs) [64, 65]. Though significant electronic conduction, which is often comparable to or higher than that of the ionic one, exists in SIMFCs, no short-circuiting nor power output loss was observed. These phenomena are obviously conflicted with conventional SOFC science and technology. Therefore, Part II deals with this especially unusual topic.



**Figure 1.22** (a, b) Mott transition makes highly electronic conductive  $SmNiO_3$  (SNO) to insulator; (c) In situ fuel cell operation makes hydrogenation of the SNO to proton-conducting electrolyte H-SNO; (d) the fuel cell performance; (e) proton conductivity of H-SNO compared to other existing proton conductors, showing excellence. Source: Reproduced with permission from Zhou et al. [61]. Copyright 2016, Springer Nature.

### 1.4.1 Fundamental Issues

In the long history of the fuel cell, fundamental understanding and scientific principles play an important role in research and development. In the first inventions, Grove had speculated that the action occurred in his gas battery at the point of contact between electrode, gas, and electrolyte, but hard to be experimentally proved due to experimental constraints. Later, researchers' work on physical properties and chemical reactions solved the puzzle of Grove's gas battery. Anyway, his exploration of the underlying chemistry of fuel cells laid the groundwork for later fuel cell researchers and science fundamentals. As a fact, argument and debate may be more important than the actual processing details. The gas battery invented by Grove in the nineteenth century spurred research and the testing of theories. While the understanding of the basic science improved, no practical device emerged despite several attempts. Work on the science of fuel cells continues, but today's work is more about developing better materials, concrete technique details with engineering, and more efficient designs, rather than discovering the basic laws and principles of science. With greater understanding of fuel cell science came attempts to make practical fuel cells. After such a long history of the fuel cell since 1839, does this mean that we do fully understand the fuel cell science and that the scope of improvements is limited? The answer to this is that there is still a need for improvements and we are not yet in line with the development work [66]. There is still a need for strong fundamental research in SOFC, especially, when shifting to lower temperatures  $<600^{\circ}\text{C}$ , and a new fundamental issue arise to overcome the sluggish electrode reaction at these temperatures.

Typically, cathode ORR process is a determining factor to develop high performance at low temperatures. Tailoring microstructures can significantly improve the SOFC cathodic performance, thus device power output [67]; this involves improvement of electron and ion pathways and triple-phase boundaries (TPB) and speed up the ORR dynamic process. The TPB is important because it is where electrons, ions, and reactants meet and electrochemical reactions occur. It is very similar to that suggested by Grove in his gas battery (fuel cell) that the action occurred at the point of contact between electrode, gas, and electrolyte. Figure 1.23 displays tailoring of the cathodic microstructure by introduction of

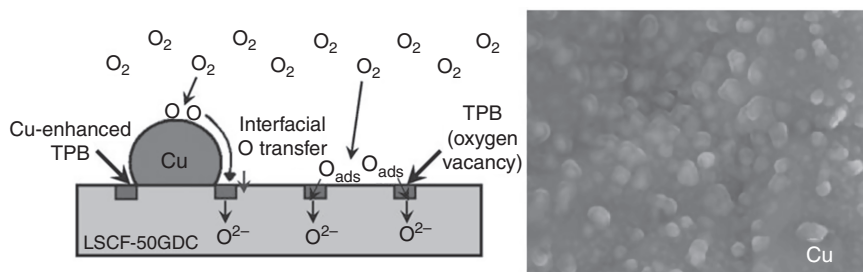


**Figure 1.23** Loading suitable metal (Cu) promoter can enhance TPB and surface oxygen vacancies and enhance more oxygen paths ways to enter the cathode, thus improving the ORR process and enhancing the device performance. Source: Guo et al. 2015 [68]. <https://www.mdpi.com/2073-4344/5/1/366>. Licensed under CC BY 4.0.

low-cost transition metal promoters, e.g. Cu, Ni, and Co. But the mechanism of metal promotion has not been fully understood, so both positive and negative promotion factors exist in literature. The loading level of transitional metal oxides has an optimum above which the interfacial oxygen transfer can be negatively influenced as the promoting nanoparticles start to obstruct the interaction sites of interfacial O with the cathode surface oxygen vacancies [68, 69].

A suitable loading of metal Cu can promote the interfacial oxygen transfer, which also enhanced TPB sites to increase  $O^{2-}$  entering the cathode and thus speed up the ORR and fuel cell performance. Otherwise, overloading or insufficient loading of Cu promoter can all make a negative effect on the device performance.

To further improve device performance to overcome critical polarization losses at the electrode side of the electrode/electrolyte interface, online redox electrode process was also proposed. Online redox process takes advantage from reduced nanometal particles, typically, Ni from nickel oxide electrodes. The fresh nanoparticles formed from the fuel cell on-site operation can possess high catalyst function, to speed up electrode redox reactions, HOR, and ORR in anode and cathode, thus significantly enhancing the fuel cell performance.

In addition, to explore SOFC multi-fuel advantage, development of redox-stable anode and cathode materials and new reaction mechanism is another important issue for multi-fuel operation and long durability of SOFCs in addition to the microstructure tailoring properties. Tao and Irvine [70] first reported redox-stable perovskite oxide,  $La_{0.75}Sr_{0.25}Cr_{0.5}Mn_{0.5}O_3$ , used for SOFC anode achieved comparable performance compared to conventional Ni-YSZ anode. In this case, it can overcome the SOFC Ni-YSZ anode instability to affect long durability problem in the steam environment because the SOFC operation produced water in the anode side. A new approach toward the SOFC configuration can be achieved with the use of amphoteric semiconductor oxides, where the same oxide will simultaneously serve the function of the cathode and anode (Figure 1.24). The latter approach is widely termed symmetrical solid oxide fuel cell (SSOFC). Some redox-stable oxides,  $La_{0.75}Sr_{0.25}Cr_{0.5}Mn_{0.5}O_3$  (LSCM) [71, 72],  $(La,Sr)(Ti_{1-x}Fe_x)O_{3-d}$  [73], and  $Sr_2Fe_{1.5}Mo_{0.5}O_{6-d}$  [26], have been reported. In this case, no anode and cathode layers were constructed

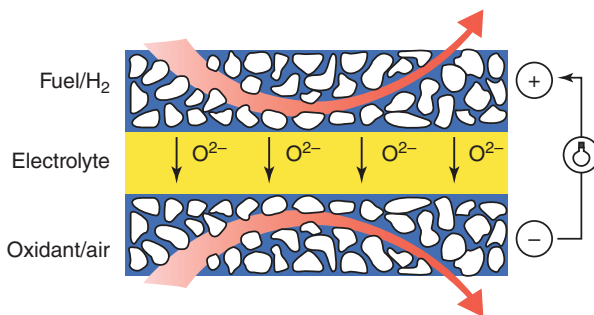


**Figure 1.24** The SOFC device constructed by the same electrode materials named as symmetrical SOFC (SSOFC).

physically by materials, but the side supplied by fuel (e.g.  $H_2$ ) or oxidant (air) determines the anode or cathode functions.

Moving to the EFFC involves science beyond very much the existing fuel cell technologies. In recent years, physical exploration of the underlying electrochemistry of EFFCs has become a fundamental field in fuel cells. The new scientific principles and fundamentals of EFFC are gradually established through the physics of semiconductors, energy bands, and semiconductor junction device technologies. The EFFC represent a disruptive fuel cell technology, which differs from the incumbent fuel cell thinking, which sometimes causes criticism toward this new technology. In this book, we shed new light on understanding the electrolyte-free or non-electrolyte technologies.

Traditional fuel cells are built around three basic components, anode, electrolyte and cathode, in which the electrolyte plays a key role for ionic transport and separating electrodes to block the electrons passing through the electrolyte, thus preventing the fuel cell of short-circuiting. A common doubt with EFFC or single-layer device is that it may be electronically short-circuited. Also, a device without a separate ionic electrolyte layer must possess a lower OCV and lower power output compared to a fuel cell with an electrolyte. In this book, we provide evidence and background understanding that EFFC can actually reach high OCVs and enhanced power output.

The fuel cell technology is, however, still subject to material and technology challenges accompanied by high costs. New material systems with very much enhanced ionic conductivity than those from the ionic designed system, e.g. YSZ and SDC, has been proposed combining ionic and semiconducting materials or semiconductors as in EFFC or deficit oxygen-defect oxides, which may achieve high power density already at temperatures well below  $600^\circ C$ , thus easing the materials and device problems. To assist and promote the SOFC solutions on challenges and commercialization, we contribute this book to give a new solution to combine the conventional SOFC technological and engineering excellence and its great advantages with new functions of the materials and devices/technologies, to speed up SOFC commercialization in a new path through.

## 1.5 Beyond the SOFC

The fuel cell development has a long history starting from the fuel cell invention in 1838. The base material of SOFC, YSZ, was discovered over 100 years ago. Though many lessons can be learned from this arch of development, this book intends to provide different ideas and new solutions beyond the existing knowledge and raise a fundamental question: are there other ways to realize the fuel cell or even not having to be the fuel cell as long as that device can realize the fuel-to-electricity conversion? Could we learn from other fields of science to bring new thinking into fuel cells? For example, the solar cell field is experiencing a highly interesting phase of development from physical p–n junction devices to electrochemical dye-sensitized and perovskite solar cells, which may complement the traditional semiconductor p–n junction-based silicon solar cell

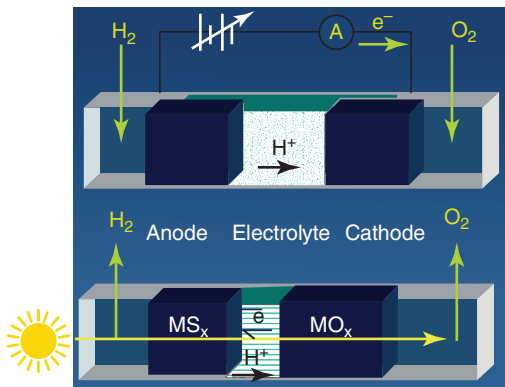


**Figure 1.25** A fuel cell generates electricity from the chemical energy of  $H_2$  and  $O_2$  and a photoelectrochemical cell produce  $H_2$  and  $O_2$  from solar radiation.

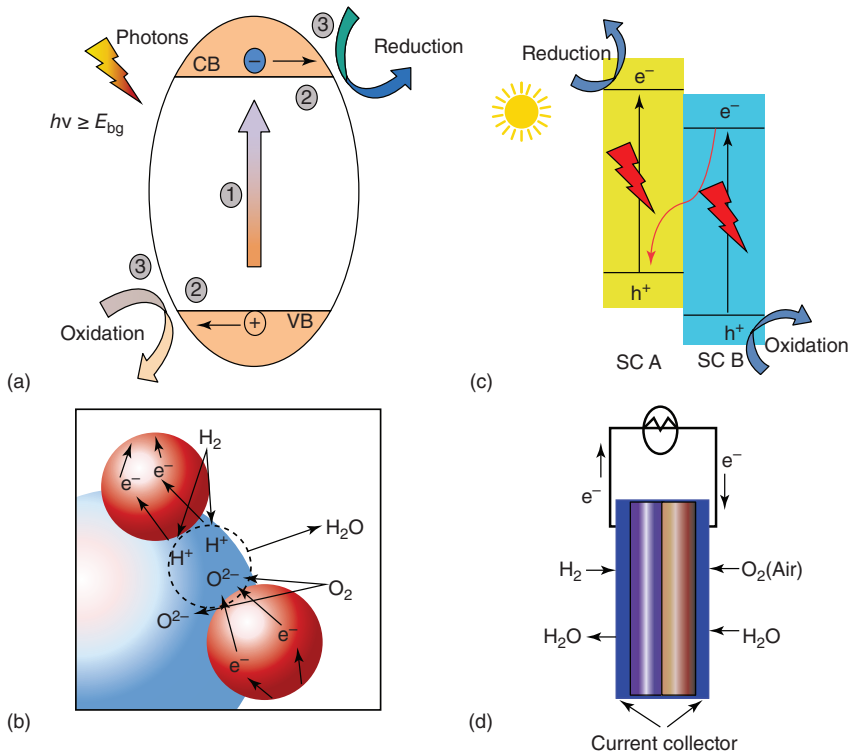


**Figure 1.26** (a, c) For photoelectrolysis realized by semiconductor band designs and the efficiency by band structure and alignment; (b) single component electrolyte-free fuel cell (EFFC) and (d) double layer EFFC devices, which are driven by the similar semiconductor principles to be described in Part II. Source: (b) Zhu et al. 2011 [57]. Reproduced with permission of Elsevier. (d) Zhu et al. 2011 [74]. Reproduced with permission of Royal Society of Chemistry.

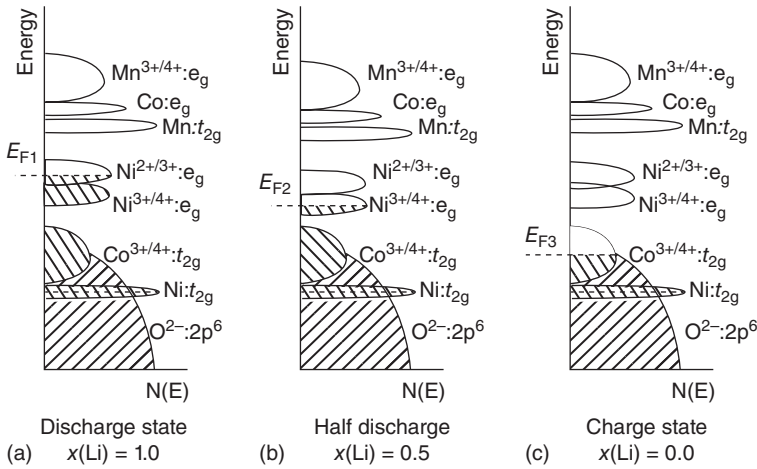


**Figure 1.27** The energy vs. density of states showing the relative Fermi level of the  $\text{Ni}_{4+/3+}$  and  $\text{Co}_{4+/3+}$  redox couples for  $\text{Li}_x\text{Ni}_y\text{Mn}_z\text{Co}_{1-2y}\text{O}_2$  during the charge, for three states of charge determined by the Li concentration  $x$ : (a)  $x = 1$ ; (b)  $x = 0.5$ ; (c)  $x = 0$ . Source: Julien et al. 2014 [77]. <https://www.mdpi.com/2304-6740/2/1/132>. Licensed Under CC BY 4.0.

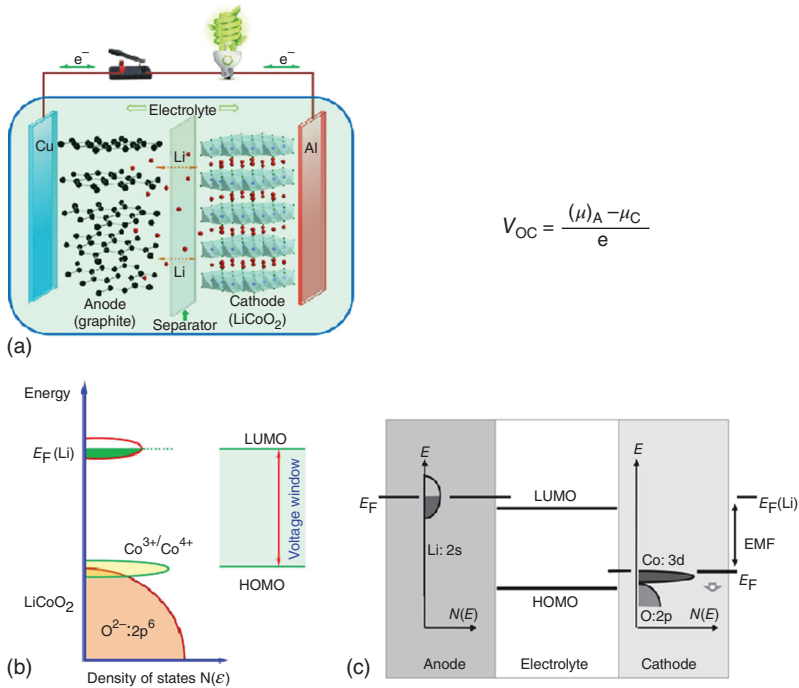


**Figure 1.28** (a) Semiconductor band structure vs. lithium battery electrochemical cell electromotive forces (EMFs). Li battery electrochemical cell. (b) Described from semiconductor energy band structures. (c) Band energy and Li battery electrochemical EMFs. Source: Reproduced with permission from Liu et al. [76]. Copyright 2016, Elsevier.

in the future. Another example may be photoelectrolysis or splitting water with photons, which were developed around the photoelectrochemical cell in the past, but today photoelectrolysis using semiconductors and band structures can be realized. Such new developments may also help fuel cells further (Figure 1.25), where similarity is shown between the fuel cell and the photoelectrochemical cells. Both are electrochemical cells. But today photoelectrolysis, semiconductor heterostructure materials are employed, in which energy band and semiconductor physics play an important role as shown in Figure 1.26. The basic mechanism and process of photocatalysis are focused on two strategies: (i) energy band modification to broaden the light absorption and (ii) surface modification (surface sensitization, semiconductor combinations, and noble metal deposition) to increase the lifetime of the carrier. All in all, the suitable band structure is the key for visible light harvesting and effective separation of the carrier of semiconductor photocatalyst. In the same way, in novel EFFCs or SLFCs, what we need is the same on charge creation, separation, transport, and reaction (“closing the circuit”), which also requires suitable band alignment. Key charges are  $h^+/e^-$  on electrodes and  $H^+$  as charge transporter. The same principle is also in EFFC.

Another good example from electrochemistry to employ very much today semiconductor band and physics is lithium battery field, which has made this field growing with a new hot area. Electrochemical performance and material properties have been now described and understood very much from semiconductor properties and band theories [75–77]. Figure 1.27 shows such an example to understand lithium battery cathode (positive) materials from semiconductor and Figure 1.28 for electrochemical cell described by band structure and physics.

The traditional electrolyte has served both as an ion conductor and as an insulator against electrons preventing short-circuiting of a fuel cell. But the short-circuiting problem could also be solved through energy band alignments and design, which have been successfully demonstrated in solar cells and photoelectrolysis, thus paving the way for the single-component EFFC. Semiconductor band and physics have made the conventional electrochemical lithium battery understood by new aspects, which have to depend on the scientific understanding and pushed the electrochemical crosslink to physics and semiconductors. Perhaps we need to look forward more openly and envision a wider range of energy applications from the new science discoveries working across the different disciplines of materials, technology, engineering, physics, and chemistry. This is a cross-thinking and philosophy beyond the fuel cell to stimulate more innovations and creations not only for future fuel cell research and development but also widely to support new advanced energy applications.

## References

- 1 Grove, W.R. (1842). On voltaic series and the combination of gases by platinum. *Philos. Mag. J. Sci.* 140: 417.
- 2 Steele, B. and Heinzl, A. (2001). Materials for fuel-cell technologies. *Nature* 414: 345.

- 3 Wilson, J.R., Kobsiriphat, W., Mendoza, R. et al. (2006). Three-dimensional reconstruction of a solid-oxide fuel-cell anode. *Nat. Mater.* 5: 541.
- 4 Haile, S.M., Boysen, D.A., Chisholm, C.R.I., and Merle, R.B. (2001). Solid acids as fuel cell electrolytes. *Nature* 410: 910.
- 5 Jacobson, M.Z., Colella, W., and Golden, D. (2005). Cleaning the air and improving health with hydrogen fuel-cell vehicles. *Science* 308: 1901.
- 6 Hibino, T., Hashimoto, A., Inoue, T. et al. (2000). A low-operating-temperature solid oxide fuel cell in hydrocarbon-air mixtures. *Science* 288: 2031.
- 7 Andersson, D., Simak, S., Skorodumova, N. et al. (2006). Optimization of ionic conductivity in doped ceria. *PNAS* 103: 3518.
- 8 Zhu, B. (2009). Solid oxide fuel cell (SOFC) technical challenges and solutions from nano-aspects. *Int. J. Energy Res.* 33: 1126.
- 9 Zhu, B. (2011). Nanocomposites for advanced fuel cell technology. *J. Nanosci. Nanotechnol.* 11: 8873.
- 10 Perry Murray, E., Tsai, T., and Barnett, S.A. (1999). A direct-methane fuel cell with a ceria-based anode. *Nature* 400: 649.
- 11 Huang, Y.H., Dass, R.I., Xing, Z.L., and Goodenough, J.B. (2006). Double perovskites as anode materials for solid-oxide fuel cells. *Science* 312: 254.
- 12 Ishihara, T., Matsuda, H., and Takita, Y. (1994). Doped LaGaO<sub>3</sub> perovskite type oxide as a new oxide ionic conductor. *J. Am. Chem. Soc.* 116: 3801.
- 13 Yang, L., Wang, S., Blinn, K. et al. (2009). Enhanced sulfur and coking tolerance of a mixed ion conductor for SOFCs: BaZr<sub>0.1</sub>Ce<sub>0.7</sub>Y<sub>0.2-x</sub>Yb<sub>x</sub>O<sub>3-δ</sub>. *Science* 326: 126.
- 14 Lacorre, P., Goutenoire, F., Bohnke, O. et al. (2000). Designing fast oxide-ion conductors based on La<sub>2</sub>Mo<sub>2</sub>O<sub>9</sub>. *Nature* 404: 856.
- 15 Goodenough, J.B., Ruiz-Diaz, J.E., and Zhen, Y.S. (1990). Oxide-ion conduction in Ba<sub>2</sub>In<sub>2</sub>O<sub>5</sub> and Ba<sub>3</sub>In<sub>2</sub>MO<sub>8</sub> (M = Ce, Hf, or Zr). *Solid State Ionics* 44: 21.
- 16 Yoshioka, H. and Tanase, S. (2005). Magnesium doped lanthanum silicate with apatite-type structure as an electrolyte for intermediate temperature solid oxide fuel cells. *Solid State Ionics* 176: 2395.
- 17 Goodenough, J.B. (2000). Ceramic technology: oxide-ion conductors by design. *Nature* 404: 821.
- 18 Kosacki, I., Rouleau, C., Becher, P. et al. (2005). Nanoscale effects on the ionic conductivity in highly textured YSZ thin films. *Solid State Ionics* 176: 1319.
- 19 Huang, H., Nakamura, M., Su, P. et al. (2007). High-performance ultrathin solid oxide fuel cells for low-temperature operation. *J. Electrochem. Soc.* 154: B20.
- 20 Shim, J.H., Chao, C.-C., Huang, H., and Prinz, F.B. (2007). Atomic layer deposition of yttria-stabilized zirconia for solid oxide fuel cells. *Chem. Mater.* 19: 3850.
- 21 Kim, K.J., Park, B.H., Kim, S.J. et al. (2016). Micro solid oxide fuel cell fabricated on porous stainless steel: a new strategy for enhanced thermal cycling ability. *Sci. Rep.* 6: 22443.
- 22 Suzuki, T., Hasan, Z., Funahashi, Y. et al. (2009). Impact of anode microstructure on solid oxide fuel cells. *Science* 325: 852.

- 23 Lee, J.G., Park, J.H., and Shul, Y.G. (2014). Tailoring gadolinium-doped ceria-based solid oxide fuel cells to achieve  $2\text{ W cm}^{-2}$  at  $550\text{ }^\circ\text{C}$ . *Nat. Commun.* 5: 4045.
- 24 Kan, W.H., Samson, A.J., and Thangadurai, V. (2016). Trends in electrode development for next generation solid oxide fuel cells. *J. Mater. Chem. A* 4: 17913.
- 25 Shao, Z.P. and Haile, S.M. (2004). A high-performance cathode for the next generation of solid-oxide fuel cells. *Nature* 431: 170.
- 26 Liu, Q., Dong, X., Xiao, G. et al. (2010). A novel electrode material for symmetrical SOFCs. *Adv. Mater.* 22: 5478.
- 27 Li, H., Tian, Y., Wang, Z. et al. (2012). An all perovskite direct methanol solid oxide fuel cell with high resistance to carbon formation at the anode. *RSC Adv.* 2: 3857.
- 28 Lan, R. and Tao, S. (2014). Novel proton conductors in the layered oxide material  $\text{Li}_x\text{Al}_{0.5}\text{Co}_{0.5}\text{O}_2$ . *Adv. Energy Mater.* 4: 1301683.
- 29 Fan, L. and Su, P.-C. (2016). Layer-structured  $\text{LiNi}_{0.8}\text{Co}_{0.2}\text{O}_2$ : a new triple ( $\text{H}^+/\text{O}^{2-}/\text{e}^-$ ) conducting cathode for low temperature proton conducting solid oxide fuel cells. *J. Power Sources* 306: 369.
- 30 Zhu, B., Fan, L., Deng, H. et al. (2016). LiNiFe-based layered structure oxide and composite for advanced single layer fuel cells. *J. Power Sources* 316: 37.
- 31 Singhal, S.C. and Kendall, K. (2003). *High-Temperature Solid Oxide Fuel Cells: Fundamentals, Design And Applications*. Elsevier.
- 32 Chadwick, A.V. (2000). Nanotechnology: solid progress in ion conduction. *Nature* 408: 925.
- 33 Zhu, B., Yang, X., Xu, J. et al. (2003). Innovative low temperature SOFCs and advanced materials. *J. Power Sources* 118: 47.
- 34 Ma, Y., Wang, X., Li, S. et al. (2010). Samarium-doped ceria nanowires: novel synthesis and application in low-temperature solid oxide fuel cells. *Adv. Mater.* 22: 1640.
- 35 Raza, R., Wang, X., Ma, Y., and Zhu, B. (2010). Study on calcium and samarium co-doped ceria based nanocomposite electrolytes. *J. Power Sources* 195: 6491.
- 36 Zhu, B. and Mat, M.D. (2006). Studies on dual phase ceria-based composites in electrochemistry. *Int. J. Electrochem. Sci.* 1: 383.
- 37 Fan, L., Wang, C., Chen, M., and Zhu, B. (2013). Recent development of ceria-based (nano)composite materials for low temperature ceramic fuel cells and electrolyte-free fuel cells. *J. Power Sources* 234: 154.
- 38 Fan, L., Zhang, G., Chen, M. et al. (2012). Proton and oxygen ionic conductivity of doped ceria-carbonate composite by modified Wagner polarization. *Int. J. Electrochem. Sci.* 7: 8420.
- 39 Xia, C., Li, Y., Tian, Y. et al. (2009). A high performance composite ionic conducting electrolyte for intermediate temperature fuel cell and evidence for ternary ionic conduction. *J. Power Sources* 188: 156.
- 40 Zhang, G., Li, W., Huang, W. et al. (2018). Strongly coupled  $\text{Sm}_{0.2}\text{Ce}_{0.8}\text{O}_2\text{-Na}_2\text{CO}_3$  nanocomposite for low temperature solid oxide fuel cells: one-step synthesis and super interfacial proton conduction. *J. Power Sources* 386: 56.

- 41 Fan, L., Zhu, B., Su, P.-C., and He, C. (2018). Nanomaterials and technologies for low temperature solid oxide fuel cells: recent advances, challenges and opportunities. *Nano Energy* 45: 148.
- 42 Raza, R., Wang, X., Ma, Y. et al. (2010). Improved ceria-carbonate composite electrolytes. *Int. J. Hydrogen Energy* 35: 2684.
- 43 Wang, X., Ma, Y., and Zhu, B. (2012). State of the art ceria-carbonate composites (3C) electrolyte for advanced low temperature ceramic fuel cells (LTCFCs). *Int. J. Hydrogen Energy* 37: 19417.
- 44 Zhu, B., Liu, X., and Schober, T. (2004). Novel hybrid conductors based on doped ceria and BCY20 for ITSOFC applications. *Electrochem. Commun.* 6: 378.
- 45 Lin, D., Wang, Q., Peng, K., and Shaw, L.L. (2012). Phase formation and properties of composite electrolyte  $\text{BaCe}_{0.8}\text{Y}_{0.2}\text{O}_{3-\delta}-\text{Ce}_{0.8}\text{Gd}_{0.2}\text{O}_{1.9}$  for intermediate temperature solid oxide fuel cells. *J. Power Sources* 205: 100.
- 46 Zhu, B., Li, S., and Mellander, B. (2008). Theoretical approach on ceria-based two-phase electrolytes for low temperature (300–600 °C) solid oxide fuel cells. *Electrochem. Commun.* 10: 302.
- 47 Wang, X., Ma, Y., Raza, R. et al. (2008). Novel core-shell SDC/amorphous  $\text{Na}_2\text{CO}_3$  nanocomposite electrolyte for low-temperature SOFCs. *Electrochem. Commun.* 10: 1617.
- 48 Shawuti, S. and Gulgun, M.A. (2014). Solid oxide-molten carbonate nano-composite fuel cells: particle size effect. *J. Power Sources* 267: 128.
- 49 Wang, X., Ma, Y., Li, S. et al. (2011). Ceria-based nanocomposite with simultaneous proton and oxygen ion conductivity for low-temperature solid oxide fuel cells. *J. Power Sources* 196: 2754–2758.
- 50 Maheshwari, A. and Wiemhöfer, H.-D. (2016). Optimized mixed ionic-electronic conductivity in two-phase ceria-zirconia composite with cobalt oxide and  $\text{Na}_2\text{CO}_3$  as suitable additives. *J. Mater. Chem. A* 4: 4402.
- 51 Maheshwari, A. and Wiemhöfer, H.-D. (2016). Augmentation of grain boundary conductivity in  $\text{Ca}^{2+}$  doped ceria-carbonate-composite. *Acta Mater.* 103: 361.
- 52 Fan, L., Ma, Y., Wang, X. et al. (2014). Understanding the electrochemical mechanism of the core-shell ceria-LiZnO nanocomposite in a low temperature solid oxide fuel cell. *J. Mater. Chem. A* 2: 5399.
- 53 Garcia-Barriocanal, J., Rivera-Calzada, A., Varela, M. et al. (2008). Colossal ionic conductivity at interfaces of epitaxial  $\text{ZrO}_2:\text{Y}_2\text{O}_3/\text{SrTiO}_3$  heterostructures. *Science* 321: 676.
- 54 Guo, X. (2009). Comment on “colossal ionic conductivity at interfaces of epitaxial  $\text{ZrO}_2:\text{Y}_2\text{O}_3/\text{SrTiO}_3$  heterostructures?”. *Science* 324: 465.
- 55 Kilner, J.A. (2008). Ionic conductors: feel the strain. *Nat. Mater.* 7: 838.
- 56 Zhu, B., Raza, R., Abbas, G., and Singh, M. (2011). An electrolyte-free fuel cell constructed from one homogenous layer with mixed conductivity. *Adv. Funct. Mater.* 21: 2465.
- 57 Zhu, B., Raza, R., Qin, H. et al. (2011). Fuel cells based on electrolyte and non-electrolyte separators. *Energy Environ. Sci.* 4: 2986.
- 58 Zhu, B., Raza, R., Qin, H., and Fan, L. (2011). Single-component and three-component fuel cells. *J. Power Sources* 196: 6362.

- 59 Zhu, B., Ma, Y., Wang, X. et al. (2011). A fuel cell with a single component functioning simultaneously as the electrodes and electrolyte. *Electrochem. Commun.* 13: 225.
- 60 Lund, P.D., Zhu, B., Li, Y. et al. (2017). Standardized procedures important for improving single-component ceramic fuel cell technology. *ACS Energy Lett.* 2: 2752.
- 61 Zhou, Y., Guan, X., Zhou, H. et al. (2016). Strongly correlated perovskite fuel cells. *Nature* 534: 231.
- 62 Dong, W., Yaqub, A., Janjua, N.K. et al. (2016). All in one multifunctional perovskite material for next generation SOFC. *Electrochim. Acta* 193: 225.
- 63 Lan, R. and Tao, S. (2015). High ionic conductivity in a  $\text{LiFeO}_2\text{-LiAlO}_2$  composite under  $\text{H}_2/\text{air}$  fuel cell conditions. *Chemistry* 21: 1350.
- 64 Cai, Y., Wang, B., Wang, Y. et al. (2018). Validating the technological feasibility of yttria-stabilized zirconia-based semiconducting-ionic composite in intermediate-temperature solid oxide fuel cells. *J. Power Sources* 384: 318.
- 65 Meng, Y., Wang, X., Xia, C. et al. (2018). High-performance SOFC based on a novel semiconductor-ionic  $\text{SrFeO}_{3-\delta}\text{-Ce}_{0.8}\text{Sm}_{0.2}\text{O}_{2-\delta}$  membrane. *Int. J. Hydrogen Energy* 43: 12697.
- 66 Connor, P.A., Yue, X., Savaniu, C.D. et al. (2018). Tailoring SOFC electrode microstructures for improved performance. *Adv. Energy Mater.* 8: 1800120.
- 67 Irvine, J., Neagu, D., Verbraeken, M. et al. (2016). Evolution of the electrochemical interface in high-temperature fuel cells and electrolyzers. *Nat. Energy* 1: 15014.
- 68 Guo, S., Wu, H., Puleo, F., and Liotta, L. (2015). B-site metal (Pd, Pt, Ag, Cu, Zn, Ni) promoted  $\text{La}_{1-x}\text{Sr}_x\text{Co}_{1-y}\text{Fe}_y\text{O}_{3-\delta}$  perovskite oxides as cathodes for IT-SOFCs. *Catalysts* 5: 366.
- 69 Liu, Y., Mori, M., Funahashi, Y. et al. (2007). Development of micro-tubular SOFCs with an improved performance via nano-Ag impregnation for intermediate temperature operation. *Electrochem. Commun.* 9: 1918.
- 70 Tao, S. and Irvine, J.T.S. (2003). A redox-stable efficient anode for solid-oxide fuel cells. *Nat. Mater.* 2: 320.
- 71 Bastidas, D.M., Tao, S., and Irvine, J.T.S. (2006). A symmetrical solid oxide fuel cell demonstrating redox stable perovskite electrodes. *J. Mater. Chem.* 16: 1603.
- 72 Ruiz-Morales, J., Canales-Vázquez, J., eña-Martínez, J. et al. (2006). On the simultaneous use of  $\text{La}_{0.75}\text{Sr}_{0.25}\text{Cr}_{0.5}\text{Mn}_{0.5}\text{O}_{3-\delta}$  as both anode and cathode material with improved microstructure in solid oxide fuel cells. *Electrochim. Acta* 52: 278.
- 73 Canales-Vázquez, J., Ruiz-Morales, J.C., Marrero-Lopez, D. et al. (2007). Fe-substituted  $(\text{La,Sr})\text{TiO}_3$  as potential electrodes for symmetrical fuel cells (SFCs). *J. Power Sources* 171: 552.
- 74 Zhu, B., Qin, H., Raza, R. et al. (2011). A single-component fuel cell reactor. *Int. J. Hydrogen Energy* 36: 8536.

- 75 Hausbrand, R., Cherkashinin, G., Ehrenberg, H. et al. (2015). Fundamental degradation mechanisms of layered oxide Li-ion battery cathode materials: Methodology, insights and novel approaches. *Mater. Sci. Eng., B* 192: 3.
- 76 Liu, C., Neale, Z.G., and Cao, G. (2016). Understanding electrochemical potentials of cathode materials in rechargeable batteries. *Mater. Today* 19: 109.
- 77 Julien, C., Mauger, A., Zaghbi, K., and Groult, H. (2014). Comparative issues of cathode materials for Li-ion batteries. *Inorganics* 2: 132.

